ACCOUNTS
of chemical research

Using Two Chemical Exchange Saturation Transfer Magnetic Resonance Imaging Contrast Agents for Molecular Imaging Studies

M. MESER ALI,[†] GUANSHU LIU,[‡] TEJAS SHAH,[§]
CHRIS A. FLASK,[§,⊥] AND MARK D. PAGEL[*,‖]

[†]Department of Radiology, Henry Ford Health System, Detroit, Michigan,
[‡]Department of Radiology, Johns Hopkins University, Baltimore, Maryland,
[§]Department of Biomedical Engineering, Case Western Reserve University,
Cleveland, Ohio, [⊥]Department of Radiology, Case Western Reserve University,
Cleveland, Ohio, [‖]Department of Chemistry and Biomedical Engineering
Interdisciplinary Program, University of Arizona, Tucson, Arizona

CONSPECTUS

Responsive magnetic resonance imaging (MRI) contrast agents can change MR image contrast in response to a molecular biomarker. Quantitative detection of the biomarker requires an accounting of the other effects that may alter MR image contrast, such as a change in the agent's concentration, magnetic field variations, and hardware sensitivity profiles. A second unresponsive MRI contrast agent may serve as an "internal control" to isolate the detection of the molecular biomarker. Chemical exchange saturation transfer (CEST) MRI

contrast agents can be selectively detected, providing the opportunity to combine a responsive CEST agent and an unresponsive CEST agent during the same MRI scan session.

When two CEST MRI contrast agents are used for molecular imaging applications, the CEST agents should be designed to maximize accurate quantification of the concentrations of the two agents. From a chemical perspective, CEST agents behave like enzymes that catalyze the conversion of an unsaturated water "substrate" into a saturated water "product". The analysis of CEST agent kinetics parallels the Michaelis−Menten analysis of enzyme kinetics, which can be used to correlate the CEST effect with the concentration of the agent in solution. If the concentration of water "substrate" that is available to the CEST agent is unknown, which may be likely for in vivo MRI studies, then only a ratio of concentrations of the two CEST agents can be measured. In both cases, CEST agents should be designed with minimal T_1 relaxivity to improve concentration quantifications.

CEST agents can also be designed to maximize sensitivity. This may be accomplished by incorporating many CEST agents within nanoparticles to create a large number of exchangeable protons per nanoparticle. Finally, CEST agents can be designed with rapid detection in mind. This may be accomplished by minimizing T_1 relaxivity of the CEST agent so that MRI acquisition methods have time to collect many MRI signals following a single selective saturation period.

In this Account, we provide an example that shows the sensitive and rapid detection of two CEST agents in an in vivo MRI study of a mouse model of mammary carcinoma. The ratio of the concentrations of the two CEST agents was quantified with analysis methods that parallel Michaelis−Menten enzyme kinetic analysis. This example demonstrates current limitations of the method that require additional research, but it also shows that two CEST MRI contrast agents can be detected and quantitatively assessed during in vivo molecular imaging studies.
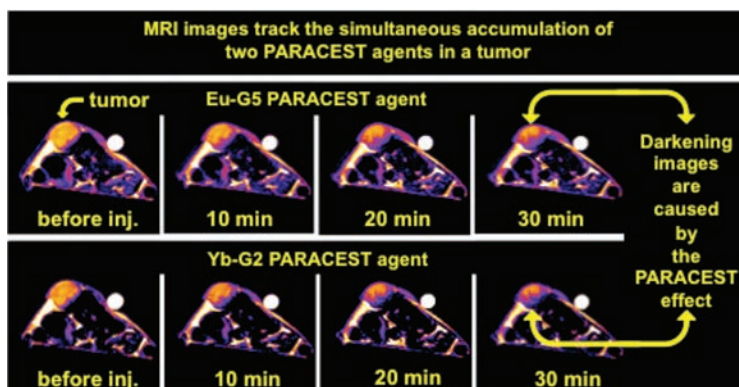
Introduction

A variety of biomedical imaging contrast agents can be designed to change image contrast in response to a molecular biomarker. However, these responsive contrast agents often respond to multiple types of molecular biomarkers or other molecular environmental conditions. In particular, pharmacokinetic processes that change the concentration of the agent in tissue can cause a change in image contrast, which compromises the assignment of changes in image contrast to a molecular biomarker. A solution to this problem involves the inclusion of a second contrast agent that is unresponsive to the molecular biomarker but is responsive to all other molecular biomarkers or molecular environmental conditions as the first agent, which is used as an "internal control agent". A comparison of the responses of both contrast agents can be used to isolate the detection of the intended biomarker. Due to variability among patients, clinical protocols, and clinical imaging hardware, the inclusion of an "internal in vivo control agent" may be particularly advantageous for translating molecular imaging to clinical practice.

A variety of responsive magnetic resonance imaging (MRI) contrast agents have been developed during the past decade that can respond to nucleic acids, proteins, enzymatic activities, redox states, metal ions, and pH.[1] Most of these contrast agents change their T_1 or T_2 relaxivities in response to a molecular biomarker, which leads to a change in image contrast. Unfortunately, the selective detection of multiple T_1 or T_2 MRI contrast agents can be a daunting challenge, because the effects of these multiple agents combine to cause a single measurement of T_1 or T_2 relaxation change. Although the selective detection of one T_1 MRI contrast agent and one T_2 MRI contrast agent is feasible, the strong correlations between T_1 and T_2 relaxation require careful calibrations to differentiate and quantify both relaxation effects.[2] Instead, the T_1 and T_2 relaxation effects can be measured from the same agent rather than from two different agents, which may be a more practical approach.[3]

As an alternative, two MRI contrast agents can be selectively detected through the mechanism of chemical exchange saturation transfer (CEST).[4] These contrast agents contain protons that undergo chemical exchange with protons of surrounding water molecules. Selective saturation of the MR signal of the proton can eliminate the MR signal of the proton. Subsequent chemical exchange of this saturated proton with a proton on a water molecule transfers the saturation to the water, which reduces the total detectable MR signal of water. Two CEST agents can have exchangeable protons with

unique chemical shifts, so that each CEST agent can be detected in the presence of other agents. Thus, two CEST MRI contrast agents may provide important advantages for quantitative molecular imaging.

Physicochemical Properties of CEST MRI Contrast Agents

An exchangeable proton on a CEST MRI contrast agent must have a unique MR chemical shift relative to the chemical shift of the same proton on a water molecule. The chemical exchange rate must be less than the difference in MR frequencies between the CEST agent and the bulk water, in order to avoid coalescence of their respective MR signals during detection. Although some diamagnetic CEST (DIACEST) agents have chemical shifts as large as 6.33 ppm (relative to the chemical shift of water that is referenced to 0 ppm), most DIACEST agents have chemical shifts of 1−4 ppm, which limits the design of CEST agents to slowly exchanging amide, amine, imine, guanidinium, indole, pyrimidine, imidazole, and alcoholic chemical groups.[4] Paramagnetic CEST (PARACEST) agents contain lanthanide ions that increase the chemical shifts of amide, amine, and alcoholic groups up to about ±50 ppm, which allows PARACEST agents to be designed with chemical groups that have much faster chemical exchange rates.[5−7] In addition, PARACEST agents can be designed to bind to a water molecule with sufficient strength that the water molecule exchanges with surrounding water at a rate that is slow enough to generate a CEST effect.[8] The proximity to the lanthanide ion can cause the bound water to resonate at CEST-detectable chemical shifts as large as 580 ppm, which further expands the chemical design of CEST agents.[9] Therefore, a wide variety CEST agents can be designed with exchangeable protons at different chemical shifts that may be selectively detected during the same MRI study.

Steady-state chemical exchange between water and an exchangeable proton on a CEST agent can be described by a two-pool model (Figure 1). The Bloch equations that describe MRI signals can be modified to include this chemical exchange, which can be used to link the effect of CEST to the physicochemical properties of the CEST agent and water (eq 1).[10] These properties include the T_1 relaxation time of the water in the presence of the agent, which is linearly dependent on the concentration of the agent (eq 2). This theory assumes that the contrast agent is completely saturated at steady state. This condition can be met for most CEST MRI contrast agents by applying selective RF saturation for a few seconds at a strong saturation power. Care must be taken to ensure that the strong saturation power is below safety lim-
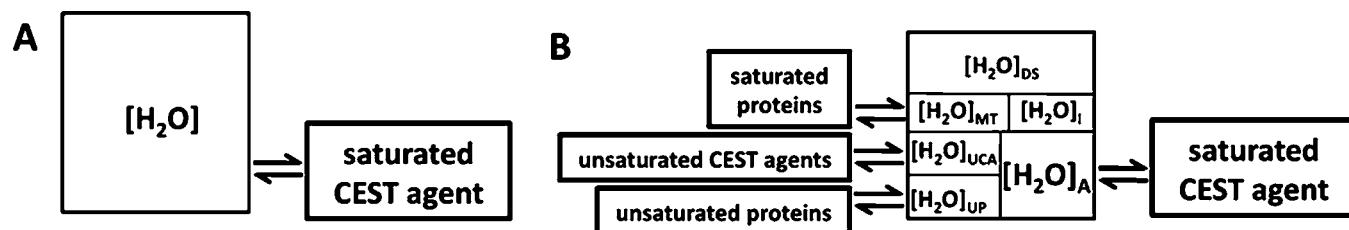
FIGURE 1. The CEST (A) two-pool model and (B) multiple-pool model. $[H_2O]_{DS}$ indicates water that is directly saturated; $[H_2O]_{MT}$ indicates water that undergoes chemical exchange with selectively saturated protein; $[H_2O]_I$ indicates water that is inaccessible to the CEST agent due to biological compartmentalization; $[H_2O]_{UCA}$ indicates water that exchanges protons with unsaturated CEST agent; $[H_2O]_{UP}$ indicates water that exchanges protons with unsaturated proteins; $[H_2O]_A$ indicates apparent water concentration that can be saturated by the saturated CEST agent.

its for in vivo studies. Care must also be taken to avoid direct saturation of bulk water, although analysis methods to account for the direct saturation of water are discussed below.

$$\frac{M_s}{M_0} = \frac{1}{1 + \dfrac{n_{CA}[CA]T_1}{n_{H_2O}[H_2O]\tau_m}} \tag{1}$$

CEST following a two-pool model

where M_s is water magnetization at steady-state selective saturation of the contrast agent, M_0 is water magnetization without saturation, n_{CA} and n_{H_2O} are the number of exchangeable protons on the contrast agent and water, $[CA]$ and $[H_2O]$ are the concentrations of contrast agent and water, T_1 is the longitudinal relaxation time of the water in the presence of the contrast agent, τ_m is the average residence lifetime of the exchangeable proton on the contrast agent, which is equal to $1/k_{ex}$ where k_{ex} is the chemical exchange rate.

$$\frac{1}{T_1} = r_1[CA] + \frac{1}{T_{1w}} \tag{2}$$

longitudinal relaxation with a contrast agent

where r_1 is the longitudinal relaxivity of the contrast agent and T_{1w} is the longitudinal relaxation time of the water without the contrast agent.

From a chemical reaction perspective, the CEST process converts water from an unsaturated "reactant" to a saturated "product". The CEST agent acts like an enzyme catalyst for this reaction, because an unsaturated proton that is transferred from water to the CEST agent is immediately saturated by MR radio frequencies, so the CEST agent is unaffected by the exchange reaction and can immediately "catalyze" the saturation of another water molecule. Although the CEST agent constantly associates with a new water molecule at a diffusion-controlled time frame of $\sim 1-10$ ns, a proton is exchanged between these molecules at a relatively slow rate of $0.2-2$ ms (i.e., the exchange is base-catalyzed or requires the metal-bound water to dissociate from the agent, which are relatively slow events). In effect, the CEST agent can be con-
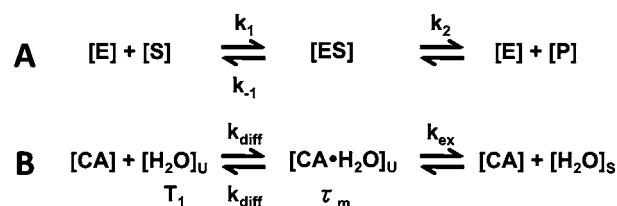

FIGURE 2. The reaction schematics of (A) Michaelis–Menten enzyme kinetics and (B) CEST are similar. Terms are defined in eqs 1, 3, and 4; n_{CA} and n_{H_2O} are omitted for clarity.

sidered to be "free" of water that can exchange a proton or "bound" to water that can exchange a proton. Thus, eq 1 that describes CEST is analogous to the Michaelis–Menten equation that describes steady-state enzyme–substrate kinetics (eq 3, Figure 2).[11] Both equations describe an experimental measurement that is a fraction of a maximum effect (i.e., M_s/M_0 and V_0/V_{max}). Both equations include a catalyst ($n_{CA}[CA]$ and $[E]$) and a reactant (unsaturated $n_{H_2O}[H_2O]$ and $[S]$). The remaining terms in eq 1 are analogous to the Michaelis dissociation constant (eq 4). Because the rate of catalysis (k_{ex}, chemical exchange rate, equivalent to k_2) is much slower than the rate of dissociation of the CEST agent and a water molecule (k_{diff}, water diffusion rate, equivalent to k_{-1}), the T_1/τ_m ratio is equivalent to $[S]/[ES]$. This is intuitive, because the T_1 relaxation time represents the time frame that the MRI-detectable water is not associated with the contrast agent ($[S]$), while the τ_m residence lifetime represents the time frame that the unsaturated water is associated with the CEST agent ($[ES]$).

$$\frac{V_0}{V_{max}} = \frac{1}{1 + \dfrac{K_M}{[S]}} \tag{3}$$

Michaelis–Menten enzyme kinetics

$$K_M = \frac{k_{-1} + k_2}{k_1} - \frac{k_{-1}}{k_1} = \frac{[E][S]}{[ES]} \quad \text{if} \quad k_{-1} \gg k_2 \tag{4}$$

the Michaelis constant

where V_0 is the initial reaction velocity for a particular $[S]$; V_{max} is the maximum reaction velocity, when $[ES] \gg [E]$; $[S]$, $[E]$, and $[ES]$ are the concentrations of substrate, enzyme, and

enzyme−substrate complex; k_1 and k_{-1} are the rates of association and dissociation of the enzyme−substrate complex, and k_2 is the rate of catalysis.

Quantification of Two CEST MRI Contrast Agents

The Michaelis−Menten equation can be analyzed in the form of the Lineweaver−Burke equation, Eadie−Hofstee equation, or Hanes equation.[12−14] The CEST equation can be similarly rearranged to form analogous linear plots (eqs 5−7, Figure 3A−C). The results of each linear analysis can be rearranged to provide a calibration of the CEST effect $(1 - M_s/M_0)$ relative to concentration of the agent (eqs 8−10, Figure 3D−F). We have previously reported the use of a Lineweaver−Burke-like CEST plot for correlating the CEST effect with the concentration of the CEST agent.[15] However, an error analysis shows that the Hanes-like CEST plot produces the most accurate results, especially for small CEST effects (Figure 3G−I).

$$\frac{1}{[CA]} = \left(\frac{1}{\frac{M_0}{M_s} - 1}\right)\left(\frac{n_{CA}T_{1w}}{n_{H_2O}[H_2O]\tau_m}\right) - r_1 T_{1w} \tag{5}$$

Lineweaver−Burke-like CEST equation

$$[CA] = \left(\frac{[CA]}{\frac{M_0}{M_s} - 1}\right)\left(\frac{n_{CA}}{n_{H_2O}[H_2O]\tau_m r_1}\right) - \frac{1}{r_1 T_{1w}} \tag{6}$$

Eadie−Hofstee-like CEST equation

$$\frac{\frac{M_0}{M_s} - 1}{[CA]} = \left(\frac{n_{CA}T_{1w}}{n_{H_2O}[H_2O]\tau_m}\right) - r_1 T_{1w}\left(\frac{M_0}{M_s} - 1\right) \tag{7}$$

Hanes-like CEST equation

$$\frac{M_s}{M_0} = \frac{1}{1 + [CA]\left(\frac{1}{m} - \frac{b[CA]}{m}\right)^{-1}} \tag{8}$$

eq 1 with the slope (m) and y-intercept (b) of eq 5

$$\frac{M_s}{M_0} = \frac{1}{1 + [CA]\left(\frac{[CA]}{m} - \frac{b}{m}\right)^{-1}} \tag{9}$$

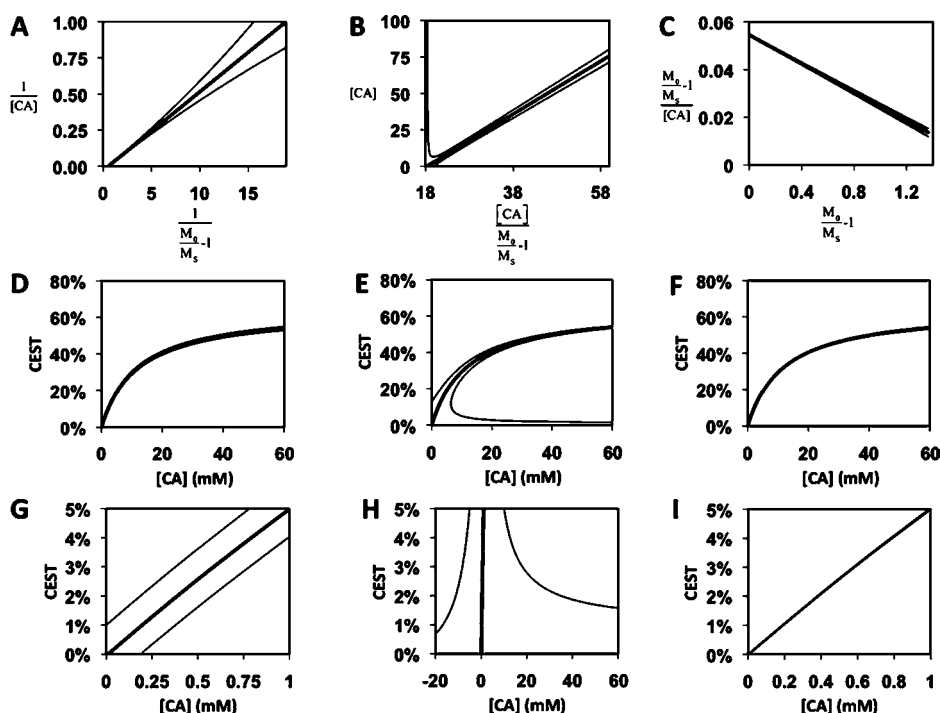eq 1 with the slope (m) and y-intercept (b) of eq 6

FIGURE 3. The (A) Lineweaver−Burke-like CEST plot, (B) Eadie−Hofstee-like CEST plot, and (C) Hanes-like CEST plot were simulated for a CEST agent that generates 5% CEST at 1 mM concentration. The thick line shows the case with no systematic error, and the thin lines represent the effect of adding +1% or −1% to the CEST measurement. (D−F) A CEST−concentration calibration can be constructed from each of these linear relationships. (G−I) The same CEST−concentration calibrations as graphs D−F, but ranging from 0 to 1 mM. These graphs show that the calibration is most accurately determined from the Hanes-like CEST plot, because the thick and thin lines are indistinguishable in graph I.

$$\frac{M_s}{M_0} = \frac{1}{1 + [CA]\left(\frac{1}{b} - \frac{m[CA]}{b}\right)^{-1}} \quad (10)$$

eq 1 with the slope (*m*) and *y*-intercept (*b*) of eq 7

The two-pool model assumes that the water pool is not directly saturated. During in vivo MRI studies, the distribution of water chemical shifts approximates a broad Lorentzian function centered at 0 ppm, so selective saturation at a chemical shift that is far from 0 ppm can still directly saturate a fraction of the water pool. Furthermore, the two-pool model can be extended to account for the presence of a second pool that represents a CEST agent that is not selectively saturated (Figure 1B).[16] This second CEST pool can exchange nonsaturated protons with the water pool, which can replenish saturated water with unsaturated protons that effectively reduces the measured CEST effect from the first CEST pool.

Despite these additional pools, the simple steady-state two-pool model can be used to empirically correlate a CEST effect with the concentration of one CEST pool while in the presence of a second CEST pool and with direct saturation of water (Figure 4).[6] These empirical correlations underestimate the CEST effect that can be calculated from the measured values of T_{1w}, r_1, τ_m, n_{CA}, [CA], and n_{H_2O}. We speculate that the empirical correlation uses a water concentration that is less than the total water concentration in the sample. Under steady-state conditions, the direct saturation of a fraction of the water pool effectively reduces the concentration of unsaturated water that can interact with the saturated CEST pool. Similarly, the unsat-

FIGURE 4. (A) The Hanes-like CEST plot and (B) CEST−concentration calibration for (C) Yb−1,4,7,10-tetraazacyclododecane-*N,N′,N″*-triacetic acid-*N‴*-orthoaminoanilide (Yb−DO3A-oAA).[6] The molecular model was constructed using CS MOPAC Pro v. 8.0 within Chem3D Ultra v. 8.0. A metal atom was inserted in the binding pocket of the model, and metal−ligand distances were constrained during final energy minimization with the MM2 force field.

urated second CEST pool effectively reduces the concentration of the unsaturated water pool that can be saturated through exchange with the saturated CEST pool. Therefore, the water concentration listed in eq 1 should be redefined as the "apparent water concentration", $[H_2O]_A$, that appears to interact with the saturated CEST pool.

The $[H_2O]_A$ may be especially difficult to determine in tissue studies. PARACEST agents are typically polar and do not easily penetrate cells. Water that remains inside cells throughout the selective saturation period will not interact with the CEST agent and is excluded from $[H_2O]_A$. Water that exchanges between intracellular and extracellular compartments during the selective saturation period will have fewer opportunities to interact with the CEST agent relative to water that remains in the extracellular compartment throughout the saturation period and therefore contributes less to $[H_2O]_A$. The pool model can be further extended to account for the presence of exchangeable protons on proteins within tissues (Figure 1B).[17] This protein pool has a broad super-Lorentzian distribution of chemical shifts that span about ±50 kHz.[18] Selective saturation within this chemical shift range will saturate a fraction of this protein pool that can exchange with the water pool. The large majority of the protein pool remains unsaturated and can exchange unsaturated protons with water and effectively reduce the measured CEST effect from the saturated CEST agent. The combination of these effects from the protein pool further reduces $[H_2O]_A$. Thus, the quantification of the absolute concentration of a saturated CEST agent in tissue may be intractable.

In vivo pharmacokinetics cause CEST agents to be heterogenously distributed within tissues. The inability of polar PARACEST agents to easily penetrate cells is one example that causes compartmentalization of the agent. The dimensions of these compartments are less than the dimensions of a MR image voxel, so the image voxel represents an average of the compartments. Because the magnitude of the CEST effect is nonlinear with respect to concentration (Figures 3D−I, Figure 4B, Figure 5C−D), the CEST effect measured from the image voxel represents the nonlinear weighted average of the CEST agent's concentration in the compartments. This nonlinear weighting causes a heterogenously distributed CEST agent to produce less CEST effect relative to a homogeneous distribution of the agent, which causes the average concentration to be underestimated. This issue reinforces that the quantification of the absolute concentration of a saturated CEST agent in tissue may be intractable.

As an alternative to measuring absolute quantifications, the quantification of the relative concentrations of two CEST
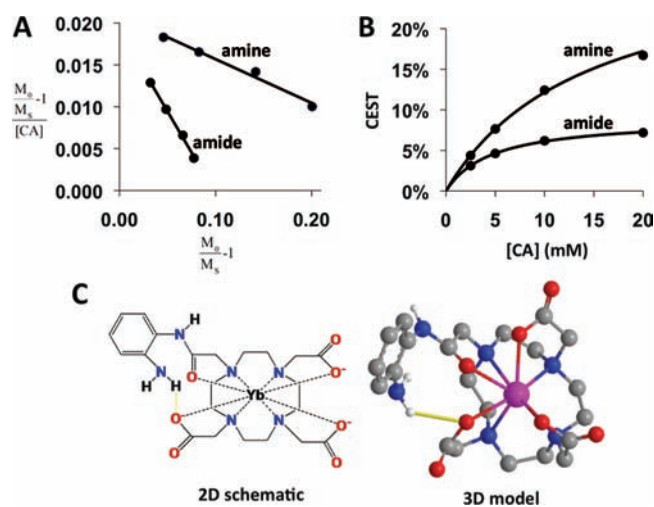
FIGURE 5. (A) The procedure for synthesizing (Yb−DOTA-Gly-pBnNCS)$_6$−G2PAMAM (Yb−G2).[24] (Eu−DOTA-Gly-pBnNCS)$_{41}$−G5PAMAM (Eu−G5) was synthesized using the same procedure. (B) A Hanes-like CEST plot was used to generate a CEST−concentration calibration (C) for Eu−G5 and (D) for Yb−G2.[23]
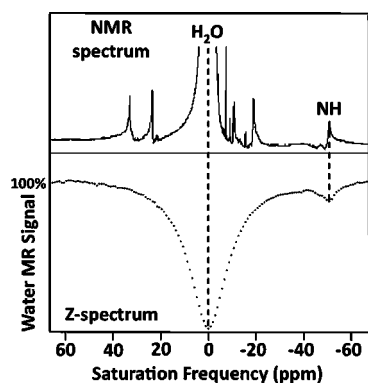

FIGURE 6. A Z-spectrum and a NMR spectrum of Tm−DOTA-Gly.

agents in tissues may be feasible. For example, if the r_1 relaxivity of two CEST agents is negligible, then the concentration ratio of two CEST agents is a simple function of their CEST effects, exchange rates, and number of exchangeable protons (eq 11). This condition is met by DIACEST agents,[19] and may also be met by PARACEST agents with low-relaxivity lanthanide ions or rapid exchange rates.[20] As another example, if two CEST agents

change their CEST effects at different linear rates while the r_1 relaxivities of both agents remain invariant, then the ratio of the time-dependent change in concentrations of the agents is a function of their CEST effects, exchange rates, and number of exchangeable protons, regardless of the magnitude of each agent's r_1 relaxivity (eq 12). Both of these functions are linear, so these analyses are not affected by heterogeneous tissue distributions of each agent, as long as the relative concentrations or relative changes in concentrations are homogeneous throughout the tissue that is represented by a MR imaging voxel. These relative quantifications rely on an equal $[H_2O]_A$ for both CEST agents. Pairs of CEST agents that have chemical shifts that are unequally distant from 0 ppm may need to account for an unequal $[H_2O]_A$ for each agent due to unequal direct saturations of water and unequal saturations of the protein pool. These systematic effects may be determined prior to injection of the CEST agents, and eqs 11 and 12 can be modified to include a constant factor that represents the

ratio of $[H_2O]_A$ for the agents. Future CEST MRI studies of tissues will be required to investigate the applicability of these ratiometric approaches.

$$\frac{[CA]_1}{[CA]_2} = \frac{\frac{\tau_m}{n_{CA_1}}\left(\frac{M_0}{M_s} - 1\right)_1}{\frac{\tau_m}{n_{CA_2}}\left(\frac{M_0}{M_s} - 1\right)_2} \quad \text{if} \quad \frac{n_{CA}}{\left(\frac{M_0}{M_s} - 1\right)n_{H_2O}[H_2O]\tau_m} \gg r_1$$

$$\text{for each agent} \quad (11)$$

$$\frac{[CA]_{1,t_2} - [CA]_{1,t_1}}{[CA]_{2,t_2} - [CA]_{2,t_1}} = \frac{\frac{n_{CA_2}}{\tau_{m,2}}\left(\frac{1}{\left(\frac{M_0}{M_s} - 1\right)_{2,t_1}} - \frac{1}{\left(\frac{M_0}{M_s} - 1\right)_{2,t_2}}\right)}{\frac{n_{CA_1}}{\tau_{m,1}}\left(\frac{1}{\left(\frac{M_0}{M_s} - 1\right)_{1,t_1}} - \frac{1}{\left(\frac{M_0}{M_s} - 1\right)_{1,t_2}}\right)}$$

$$(12)$$

where x = type of contrast agent and t_y = time point for $[CA]_{x,t_y}$ and $(M_0/M_s - 1)_{x,t_y}$ and

$$\frac{\frac{1}{[CA]_{2,t_1}} - \frac{1}{[CA]_{2,t_2}}}{\frac{1}{[CA]_{1,t_1}} - \frac{1}{[CA]_{1,t_2}}} = \frac{[CA]_{1,t_2} - [CA]_{1,t_1}}{[CA]_{2,t_2} - [CA]_{2,t_1}}$$

if $[CA]_{x,t_0} = 0$ and changes in concentration are linearly dependent on time.

Sensitivity of CEST MRI Contrast Agents

A concentration of 1−10 mM of a small molecule CEST agent is typically required to generate a 5% CEST effect. Chemical designs have been demonstrated that increase k_{ex} and improve the CEST sensitivity.[21] But k_{ex} must be less than the chemical shift of the contrast agent, so efforts to increase k_{ex} to improve CEST sensitivity are inherently limited. Chemical designs that reduce or eliminate r_1 relaxivity can also improve CEST sensitivity. But the T_1 relaxation time of the water with the agent must be no greater than the T_1 relaxation time of the water without the agent, so efforts to eliminate r_1 relaxivity to improve CEST sensitivity are also inherently limited. Inspection of eq 1 shows that the only remaining parameter that can be exploited to improve CEST MRI sensitivity is the number of exchangeable protons per molecule.

Dendrimers can be used as a nanocarrier to transport many PARACEST contrast agents.[22] We have developed polyamidoamine (PAMAM) dendrimers that carry many PARACEST agents to demonstrate the utility of dendrimers for boosting PARACEST sensitivity.[23] DOTA-Gly with an isothiocyanatoben-

zyl group (S-2-(4-isothiocyanatobenzyl)-1,4,7,10-tetraazacyclododecane-tetraacetic acid) was conjugated to the surface amine groups of a generation-5 PAMAM (G5PAMAM) dendrimer to generate (DOTA-Gly-pBnNCS)$_{41}$−G5PAMAM (Figure 5A) following a recently published method.[24] This product was then used to chelate Eu(III) to create (Eu−DOTA-Gly-pBnNCS)$_{41}$−G5PAMAM, which generated a PARACEST effect from the metal-bound water. A similar procedure was used to create (Yb−DOTA-Gly-pBnNCS)$_6$−G2PAMAM, which generated a PARACEST effect from the amides of the chelate. A Hanes-like calibration plot was used to correlate the CEST effect with concentration for each dendrimer (Figure 5C). These results showed that 79.8 μM of (Eu−DOTA-Gly-pBnNCS)$_{41}$−G5PAMAM and 335.5 μM of (Yb−DOTA-Gly-pBnNCS)$_6$−G2PAMAM can each generate a 5% CEST effect.

Temporal Resolution for Detecting CEST MRI Contrast Agents

The characterization of a chemical solution of a CEST agent often employs the acquisition of a Z-spectrum, which shows the dependence of the water MR signal on selective saturation at each MR spectral frequency (Figure 6).[25] Each selective saturation can require 2−4 s to ensure complete saturation of the CEST agent, which requires a reasonable ~3−13 min to acquire a Z-spectrum of ~50−200 MR saturation frequencies. In practice, multiple signal acquisitions are acquired at each MR frequency of the Z-spectrum to reduce artifacts through phase cycling, to improve the signal-to-noise ratio, or to acquire spatial information for a MR image. These multiple acquisitions can cause total CEST MRI experiments to exceed 1 hour in length, which is impractical for many in vivo studies. Moreover, the comparison of two CEST agents may require rapid detection of each agent to properly assess biomarkers.[26]

We have developed two approaches to improve the temporal resolution for acquiring multiple CEST MR images.[27] The first approach acquires a temporal series of CEST MR images with selective saturation at only one MR frequency and monitors the change in CEST contrast before and after i.v. injection of the contrast agent. This dynamic contrast CEST MRI study is not affected by static conditions such as direct saturation of water, the magnetization transfer effect, and magnetic field inhomogeneities. Yet this approach cannot account for dynamic changes in magnetic susceptibilities and water T_2 relaxation that are caused by the CEST agent, which can dynamically alter the direct saturation of water. Therefore, this approach is only appropriate for PARACEST agents with large
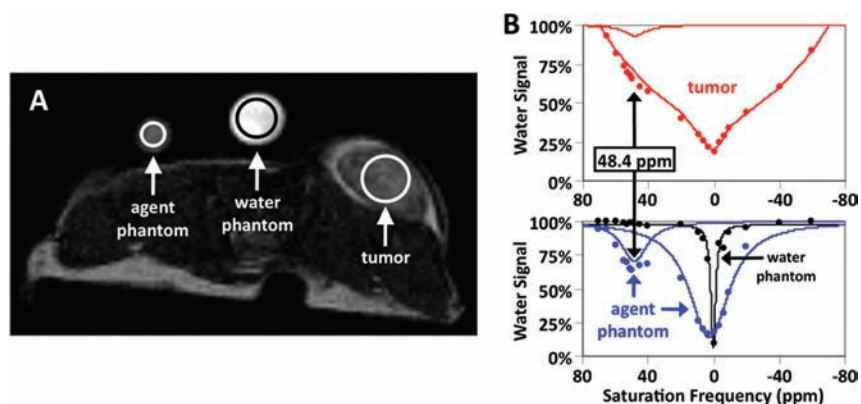
FIGURE 7. (A) A spin density weighted MR image of a MCF-7 tumor on a mouse flank, with phantoms of 40 mM (Eu−DOTA-Gly)$_{41}$−G5PAMAM contrast agent and water.[28] (B) Fifty microliters of 40 mM (Eu−DOTA-Gly)$_{41}$−G5PAMAM was directly injected into the tumor. Twenty CEST−FISP MRI images with a range of saturation frequencies were acquired with a 20 μT saturation period for 2.25 s prior to a FISP MRI acquisition. Z-spectra were constructed from the CEST effect in each displayed image region. To account for magnetization transfer effects, the right side of the Z-spectrum of the tumor was interpolated and mirrored to the left side of the spectrum. This interpolation method is affected by the data sampling, so this analysis method only approximates magnetization transfer effects. Lorentzian line-fitting of each spectrum revealed that the CEST effects from the tumor and agent phantom both occurred at 48.4 ppm. The total acquisition required 200 s.

chemical shifts that show little or no influence from these dynamic effects.

Two types of MRI pulse schemes may be used to perform dynamic contrast CEST MRI. A rapid multiple-echo acquisition scheme (such as a rapid acquisition with relaxation enhancement (RARE) MRI scheme) following the selective saturation can be used to collect many or all of the MR signals that are needed to construct an image before selective saturation must be repeated to maintain steady-state CEST conditions. This approach works well if the T_1 relaxation time of the water in the presence of the contrast agent is relatively long (e.g., greater than 2 s) so that the CEST effect is not appreciably reduced by T_1 relaxation during the long acquisition scheme. This scheme can generate a MR image with CEST contrast within 5 s, which can be repeated with selective saturation at other MR frequencies in order to detect two CEST agents. Alternatively, if the T_1 relaxation time is short, only a short single-echo acquisition scheme following the selective saturation can be used to collect a single MR signal before the CEST effect is reduced by T_1 relaxation. In this case, single-echo acquisitions (such as a fast low-angle shot (FLASH) MRI scheme) can be interleaved with short saturation periods to generate a MR image with CEST contrast within 13 s.

Our second approach for improving temporal resolution acquires a series of CEST MR images with selective saturation at each MR frequency of the Z-spectrum.[28] These MR frequencies are carefully chosen to provide fine spectral resolution about the chemical shifts of the CEST agent and water and coarse resolution throughout the remainder of the spectrum. Spectral analysis routines can then be used to effec-

tively interpolate the experimental data to produce high-quality Z-spectra for each image pixel.[29] The multiple MR images that are required for this approach must be acquired very rapidly to retain reasonable temporal resolution. Thus, this approach requires a multiple-echo acquisition scheme. We have employed a CEST−fast imaging with a steady state free precession (FISP) MRI acquisition method to acquire CEST images with a temporal resolution as low as 3 s to obtain the 20-point MR CEST spectroscopic image of a xenograft mouse model of mammary carcinoma that was injected with a PARACEST agent (Figure 7). This example demonstrates that the CEST MR spectroscopic image may be obtained within 200 s for each CEST agent.

Examples of Detecting Two CEST MRI Contrast Agents

The powerful utility of detecting two CEST effects within a single sample was immediately apparent during the discovery of this MRI phenomenon.[19] The chemical exchange rates of amide, amine, and imine chemical functional groups have different dependencies on pH, so the ratio of the DIACEST effects from two of these functional groups can be used to measure a part of the range of physiological pH. We have exploited this approach to create a PARACEST agent with an amide and aryl amine chemical group that can measure the entire physiological pH range with an improved dynamic range relative to pH-dependent DIACEST agents.[30] The amide of this agent shows base-catalyzed chemical exchange behavior throughout the physiological pH range, which causes an increase in PARACEST from the amide with respect to increasing pH. The aryl

amine of this agent shows base-catalyzed chemical exchange behavior below a pK_a of 7.1 and acid-catalyzed chemical exchange behavior above this pK_a. The combination of these chemical exchange mechanisms causes PARACEST of the aryl amine to be less dependent on pH relative to PARACEST from the amide. In effect, the PARACEST from the aryl amine serves as an "internal control" relative to the pH-dependent PARACEST from the amide, so that this agent can be used to measure pH without needing to account for other affects that change image contrast such as the concentration of the agent.

We have utilized two PARACEST agents in solution, in order to detect enzymatic activity.[15] Our enzyme-responsive agent contains a peptidyl ligand that is cleaved by caspase-3, which causes the amide at the scissile bond to be converted to an amine. Although the CEST effect of the amine in the reaction product can be detected, its small chemical shift and weak CEST effect are impractical for in vivo studies. Instead, the CEST effect of the amide can be easily detected to monitor the enzyme reaction. Yet the absence of contrast after enzyme cleavage is a flawed approach for detecting a biomarker because the lack of a CEST effect may be due to many factors other than enzymatic activity. To overcome this flaw, we have included a second enzyme-unresponsive PARACEST agent in the sample that acts as an internal control. The ratio of the CEST effects from both agents validates the detection of enzymatic activity. To translate this approach to in vivo studies, the two PARACEST agents should be linked to the same nanocarrier such as a dendrimer so that the ratio of their concentrations is not affected by different in vivo pharmacokinetics for two separate agents.

Two paramagnetic liposomal-based CEST MRI contrast agents have recently been detected in the same location of ex vivo tissue.[31] We have extended this approach to in vivo tissues by detecting two PARACEST agents within the same tumor tissue in a mouse model of mammary carcinoma.[32] This demonstration required consideration for quantification, sensitivity, and temporal resolution for detecting two CEST MRI contrast agents, as discussed in the previous sections. The dendritic PARACEST agents (Eu−DOTA-Gly-pBnNCS)$_{41}$−G5PAMAM and (Yb−DOTA-Gly-pBnNCS)$_6$−G2PAMAM were injected i.v. into a mouse model of MCF-7 mammary carcinoma. Because the tumor tissue has a relatively long T_1 relaxation time of approximately 2.5 s, a multiple-echo CEST−RARE MRI acquisition scheme was used to detect each agent within the tumor (Figure 8A). The decrease in MR signal of the tumor after injection relative to the average MR signal before injection was used to measure the temporal change in the CEST effect (Figure 8B).
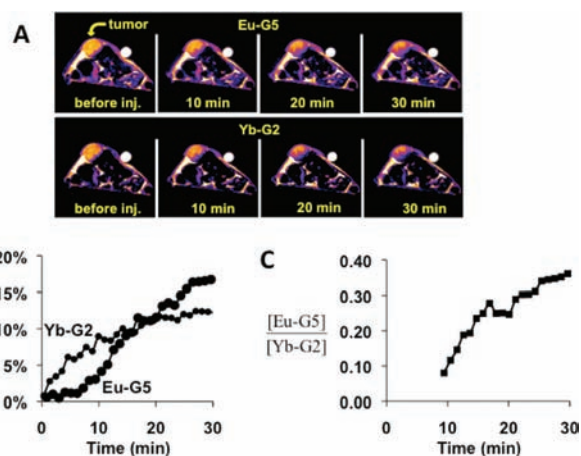

FIGURE 8. (Eu−DOTA-Gly)$_{41}$−G5PAMAM (Eu−G5) and (Yb−DOTA-Gly)$_6$−G2PAMAM (Yb−G2) were injected i.v. at 0.03 mmol of dendrimer per kilogram of mouse body weight into a xenograft flank mouse model of MCF-7 mammary carcinoma.[32] (A) MR images were acquired by prepending a 20 μT saturation period for 2.25 s before a RARE-16 MR signal acquisition period. Selective saturation was applied at the PARACEST frequency of each agent. (B) The decrease in MR signal of the tumor after injection relative to the average MR signal before injection was used to measure the temporal change in the CEST effect. (C) Equation 11 was used to calculate the concentration ratio of the CEST agents.

Equation 11 was used to calculate the concentration ratio of the CEST agents (Figure 8C). The condition listed in eq 11 is valid for (Eu−DOTA-Gly-pBnNCS)$_{41}$−G5PAMAM, but this condition is questionable for (Yb−DOTA-Gly-pBnNCS)$_6$−G2PAMAM if the CEST effect and $[H_2O]_A$ are high, due in part to the greater r_1 relaxivity of ytterbium relative to europium. In addition, eq 11 assumes that $[H_2O]_A$ is the same for both agents. This assumption is not valid, because $[H_2O]_{DS}$ and $[H_2O]_{MT}$ are different for each agent due to the different saturation frequencies of each agent, and $[H_2O]_{UCA}$ is different for both agents due to different pharmacokinetics of each agent. Additional investigations are required to understand the relationship between in vivo $[H_2O]_A$ for each CEST agent. Yet the concentration ratio correctly shows that the lower tissue permeability of the larger dendrimer causes a fraction of (Eu−DOTA-Gly-pBnNCS)$_{41}$−G5PAMAM to accumulate in the tumor tissue relative to (Yb−DOTA-Gly-pBnNCS)$_6$−G2PAMAM, and the lower elimination rate of the larger dendrimer causes this fraction to increase over time. With similar considerations for quantification, sensitivity, and temporal resolution, other examples of two CEST MRI contrast agents may be developed for preclinical molecular imaging studies and translation of quantitative molecular imaging to the clinic.

BIOGRAPHICAL INFORMATION

M. Meser Ali received his Ph.D. degree in Organometallic Chemistry from the University of Mie in Japan in 1999. He conducted postdoctoral research with Ronald Elsenbaumer at the University of Texas at Arlington, A. Dean Sherry at the University of Texas at Dallas, and Mark Pagel at Case Western Reserve University. He is an Instructor in the Department of Radiology at Henry Ford Health System, Detroit, Michigan. His research program focuses on the development of "smart" nanoparticle platforms for both cancer therapy and imaging.

Guanshu Liu received his Ph.D. degree in biomedical engineering from Case Western Reserve University in 2008 under the supervision of Mark Pagel. He is currently performing postdoctoral research at the Johns Hopkins University, where his research investigates the development of MRI contrast agents for cell labeling and drug delivery.

Tejas Shah received his M.S. degree in Biomedical Physics and BioEngineering from University of Aberdeen, U.K., in 2004. He is currently working towards a Ph.D. degree in biomedical engineering from Case Western Reserve University under the supervision of Chris Flask. His is currently studying the effect of CEST from glycogen.

Chris A. Flask received his Ph.D. degree in biomedical engineering from Case Western Reserve University in 2005. Dr. Flask is an Assistant Professor of Radiology and Biomedical Engineering at Case Western Reserve University. His research interests focus on the development of quantitative MRI techniques to characterize hepatic and renal diseases such as fibrosis, fatty liver disease, and polycystic kidney disease.

Mark "Marty" Pagel received his Ph.D. degree in chemistry from the University of California, Berkeley, in 1993. He began his research studies of CEST MRI contrast agents at Case Western Reserve University in 2003, and he has recently moved to the University of Arizona in 2008 to take a position as an Associate Professor of Chemistry and Biomedical Engineering. His research investigates the development of MRI contrast agents for molecular studies of cancer therapies.

REFERENCES

1 Yoo, B.; Pagel, M. D. An overview of responsive MRI contrast agents for molecular imaging. *Front. Biosci.* **2008**, *13*, 1733–1752.

2 Zhang, X.; Martinez, G. V.; Garcia-Martin, M. L.; Woods, M.; Sherry, A. D.; Gillies, R. J. In vivo pHe measurement with a relaxometric pH sensitive contrast agent. *Proc. World Mol. Imaging Congr.* **2008**, 0481.

3 Aime, S.; Fedeli, F.; Sanino, A.; Terreno, E. A R_2/R_1 ratiometric procedure for a concentration-independent, pH-responsive, Gd(III)-Based MRI agent. *J. Am. Chem. Soc.* **2006**, *128* (35), 11326–11327.

4 Ward, K. M.; Aletras, A. H.; Balaban, R. S. A new class of contrast agents for MRI based on proton chemical exchange dependent saturation transfer (CEST). *J. Magn. Reson.* **2000**, *143*, 79–87.

5 Zhang, S.; Michaudet, L.; Burgess, S.; Sherry, A. D. The amide protons of an ytterbium(III) dota tetraamide complex act as efficient antennae for transfer of magnetization to bulk water. *Angew. Chem., Int. Ed.* **2002**, *41* (11), 1919–1921.

6 Liu, G.; Lu, Y.; Pagel, M. D. Design and characterization of a new irreversible responsive PARACEST MRI contrast agent that detects nitric oxide. *Magn. Reson. Med.* **2007**, *58*, 1249–1256.

7 Woods, M.; Woessner, D. E.; Zhao, P.; Pasha, A.; Yang, M. Y.; Huang, C. H.; Vasalitiy, O.; Morrow, J. R.; Sherry, A. D. Europium(III) macrocyclic complexes with alcohol pendant groups as chemical exchange saturation transfer agents. *J. Am. Chem. Soc.* **2006**, *128*, 10155–10162.

8 Zhang, S.; Winter, P.; Wu, K.; Sherry, A. D. A novel europium(III)-based MRI contrast agent. *J. Am. Chem. Soc.* **2001**, *123*, 1517–1518.

9 Terreno, E.; Delli Castelli, D.; Cravotto, G.; Milone, L.; Aime, S. Ln(III)-DOTAMGly complexes: A versatile series to assess the determinants of the efficacy of paramagnetic chemical exchange saturation transfer agents for magnetic resonance imaging applications. *Invest. Radiol.* **2004**, *39*, 235–243.

10 Zhang, S.; Merritt, M.; Woessner, D. E.; Lenkinski, R. E.; Sherry, A. D. PARACEST agents: Modulating MRI contrast via water proton exchange. *Acc. Chem. Res.* **2003**, *36*, 783–790.

11 Briggs, G. E.; Haldane, J. B. A note on the kinetics of enzyme action. *Biochem. J.* **1925**, *19* (2), 338–339.

12 Hanes, C. S. Studies on plant amylases: The effect of starch concentration upon the velocity of hydrolysis by the amylase of germinated barley. *Biochem. J.* **1932**, *26* (5), 1406–1421.

13 Lineweaver, H.; Burk, D. Determination of enzyme dissociation constants. *J. Am. Chem. Soc.* **1934**, *56*, 658–666.

14 Hofstee, B. H. On the evaluation of the constants Vm and KM in enzyme reactions. *Science* **1952**, *116* (3013), 329–331.

15 Yoo, B.; Raam, M.; Rosenblum, R.; Pagel, M. D. Enzyme-responsive PARACEST MRI contrast agents: A new biomedical imaging approach for studies of the proteasome. *Contrast Media Mol. Imaging* **2007**, *2*, 189–198.

16 Woessner, D. E.; Zhang, S.; Merritt, M. E.; Sherry, A. D. Numerical solution of the Bloch equations provides insights into the optimum design of PARACEST agents for MRI. *Magn. Reson. Med.* **2005**, *53*, 790–799.

17 Li, A. X.; Hudson, R. H. E.; Barrett, J. W.; Jones, C. K.; Pasternak, S. H.; Bartha, R. Four-pool modeling of proton exchange processes in biological systems in the presence of MRI-paramagnetic chemical exchange saturation transfer (PARACEST) agents. *Magn. Reson. Med.* **2008**, *60*, 1197–1206.

18 Henkelman, R. M.; Stanisz, G. J.; Graham, S. J. Magnetization transfer in MRI: A review. *NMR Biomed.* **2001**, *14*, 57–64.

19 Ward, K. M.; Balaban, R. S. Determination of pH using water protons and chemical exchange dependent saturation transfer. *Magn. Reson. Med.* **2000**, *44*, 799–802.

20 Aime, S.; Barge, A.; Delli Castelli, D.; Fedeli, F.; Mortillaro, A.; Nielsen, F. U.; Terreno, E. Paramagnetic lanthanide(III) complexes as pH-sensitive chemical exchange saturation transfer (CEST) contrast agents for MRI applications. *Magn. Reson. Med.* **2002**, *47*, 639–648.

21 Ratnakar, S. J.; Woods, M.; Lubag, A. J. M.; Kovacs, Z.; Sherry, A. D. Modulation of water exchange in europium(III) DOTA-tetraamide complexes via electronic substituent effects. *J. Am. Chem. Soc.* **2008**, *130*, 6–7.

22 Pikkemaat, J. A.; Wegh, R. T.; Lamerichs, R.; van de Molengraaf, R. A.; Sangereis, S.; Burdinski, D.; Raymond, A. Y. F.; Janssen, H. M.; de Waal, B. F. M.; Willard, N. P.; Meijer, E. W.; Grull, H. Dendritic PARACEST contrast agents for magnetic resonance imaging. *Contrast Media Mol. Imaging* **2007**, *2*, 229–239.

23 Ali, M.; Pagel, M. D. Improved assessments of breast cancer with DCE-MRI using two dendritic PARACEST agents. *Proc. Soc. Mol. Imaging* **2007**, 0598.

24 Ali, M. M.; Woods, M.; Caravan, P. C.; Opina, A.; Spiller, A.; James, C.; Sherry, A. D. Synthesis and relaxometric studies of a dendrimer-based pH responsive MRI contrast agent. *Chem.—Eur. J.* **2008**, *14*, 7250–7258.

25 Bryant, R. D. The dynamics of water-protein interactions. *Annu. Rev. Biophys. Biomol. Struct.* **1996**, *25*, 29–53.

26 Shapiro, M.; Atanasijevic, T.; Faas, H.; Westmeyer, G.; Jasanoff, A. Dynamic imaging with MRI contrast agents: quantitative considerations. *Magn. Reson. Imaging* **2006**, *24* (4), 449–462.

27 Liu, G.; Ali, M. M.; Yoo, B.; Griswold, M. A.; Tkach, J. A.; Pagel, M. D. PARACEST MRI with improved temporal resolution. *Magn. Reson. Med.* **2008**, *61*, 399–408.

28 Shah, T.; Ali, M. M.; Liu, G.; Pagel, M. D.; Flask, C. A. FISPCEST: A rapid acquisition for dynamic detection of CEST/PARACEST activity. *Proc. Int. Soc. Magn. Reson. Med.* **2008**, 3067.

29 Stancanello, J.; Terreno, E.; Delli Castelli, D.; Cabella, C.; Uggeri, F.; Aime, S. Development and validation of a smoothing-splines-based correction method for improving the analysis of CEST-MR images. *Contrast Media Mol. Imaging* **2008**, *3* (4), 136–149.

30 Liu, G.; Li, Y.; Pagel, M. D. A new class of PARACEST MRI contrast agents for in vivo pH measurements. *Proc. Soc. Mol. Imaging* **2007**, 0325.

31 Terreno, E.; Delli Castelli, D.; Milone, L.; Rollet, S.; Stancanello, J.; Violante, E.; Aime, S. First ex-vivo MRI co-localization of two LIPOCEST agents. *Contrast Media Mol. Imaging* **2008**, *3*, 38–43.

32 Ali, M. M.; Yoo, B.; Pagel, M. D. Tracking the relative in vivo pharmacokinetics of nanoparticles with PARACEST MRI. *Mol. Pharmaceutics*, published online March 19, **2009**, DOI: 10.1021/mp900040u.